

# THE EFFECT OF THE LOAD BEARING AREA ON THE HIGH CYCLE FATIGUE LIMIT IN HIGH DENSITY SINTERED LOW ALLOYED STEELS

C. Xu\*, G. Khatibi\*\*, B. Weiss\*\*, H. Danninger\*

\* Institute of Chemical Technologies and Analytics in Tech. Univ. of Vienna

\*\* Institute of Materials Physics in Vienna Univ.

E164 Institute of Chemical Technologies and Analytics

Getreidemarkt 9/164-CT

1060 Wien

Austria

e-mail: [chenxu@mail.zserv.tuwien.ac.at](mailto:chenxu@mail.zserv.tuwien.ac.at)

## Abstract

Many studies have been carried out to find a relationship between the fatigue limit and the porosity in sintered materials. It seems that the fatigue limit cannot be adequately described only by variables pertinent to the complex pore structure. Another set of variables that are pertinent to the matrix may also be significant in fatigue life modeling. The load bearing area is the true area where the fatigue stress acts in sintered steels. It may be a suitable parameter. In order to investigate the influence of the load bearing area on HCF life, the fatigue limits were measured on specimens of low alloy sintered steel Fe-1.5Cr-0.2Mo-0.6C and Fe-1.5Mo-0.6C prepared from prealloyed Fe-Cr-Mo and Fe-Mo powders. The specimens were produced by the press-and-sinter route as common for powder metallurgy precision parts. The density of the specimens ranged from 7.1g/cm<sup>3</sup> to 7.5g/cm<sup>3</sup>, respectively, the corresponding residual porosity range being from 10% to 4%. Sintering was done at temperatures of 1120°C. Fatigue testing was carried out using a 20 kHz ultrasonic resonance system that operates in a push-pull mode at R=-1. The maximum cycle number was 10E9. Specially adapted image analyzing software was used to determine the load bearing area on the fracture surface of these specimens. The relationship between fatigue limit, ultimate tensile strength and the load bearing area is discussed.

## 1. Introduction

Sintered low alloyed steels are outstandingly important for precision parts in the automotive industry, esp. for engines and transmissions. These applications of sintered steels are frequently high cycle fatigue applications. A characteristic feature of sintered steels is that they may contain various amounts of porosity which does not exist in wrought

steels products. In wrought steels, a number of models have been developed to predict the fatigue life based on the inclusion size. The predictive capability of the models has been shown to be very adequate Laz, et al [8]. However, in sintered steels, the models based on the pore structure only behaved poorly on the fatigue life prediction Weiss, et al[1]. The reason is largely that the complexity of the pores in the sintered materials is much more significant than the microstructural defects in wrought materials.

It has been pointed out by several investigators that the pores in the microstructure of sintered steels may appear isolated, interconnected, or a mixture of both and the effects of pores on fatigue properties are not only porosity but also pore size, shape, connectivity, distribution, and location. For the above-mentioned reasons, some investigators proposed to consider the interparticle bridge area of solid phase, the load bearing area  $A_c$ , as a parameter for the fatigue properties rather than the pores. The load bearing area is that area where mechanical loading acts in sintered steels (pores do not bear any load). This parameter can be measured on fracture surfaces by SEM fractographic techniques using an image analysis system. A relationship between fatigue limit and the load bearing area in some sintered materials was proposed by Danninger et al [2].

In this paper a new image analyzing program was developed to determine the load bearing area in the fracture surface of specimens. The program is used to evaluate the fracture surface of low alloy PM steel Astaloy CrL(Fe-1.5Cr-0.2Mo) + 0.6C and Astaloy Mo(Fe-1.5Mo)+0.6C. The density levels of the specimens range from 7.1g/cm<sup>3</sup> to 7.5g/cm<sup>3</sup>. Sintering was done at 1120°C. Fatigue testing was carried out using a 20 kHz ultrasonic resonance system that operates in a push-pull mode at R=-1. In our evaluation the fatigue limits were taken as the stress amplitudes corresponding to the 50% fracture probability at N = 1.0E09. By analyzing the results, relationships between fatigue limit, ultimate tensile strength, and  $A_c$  were discussed.

## 2. Experimental

### 2.1. Materials

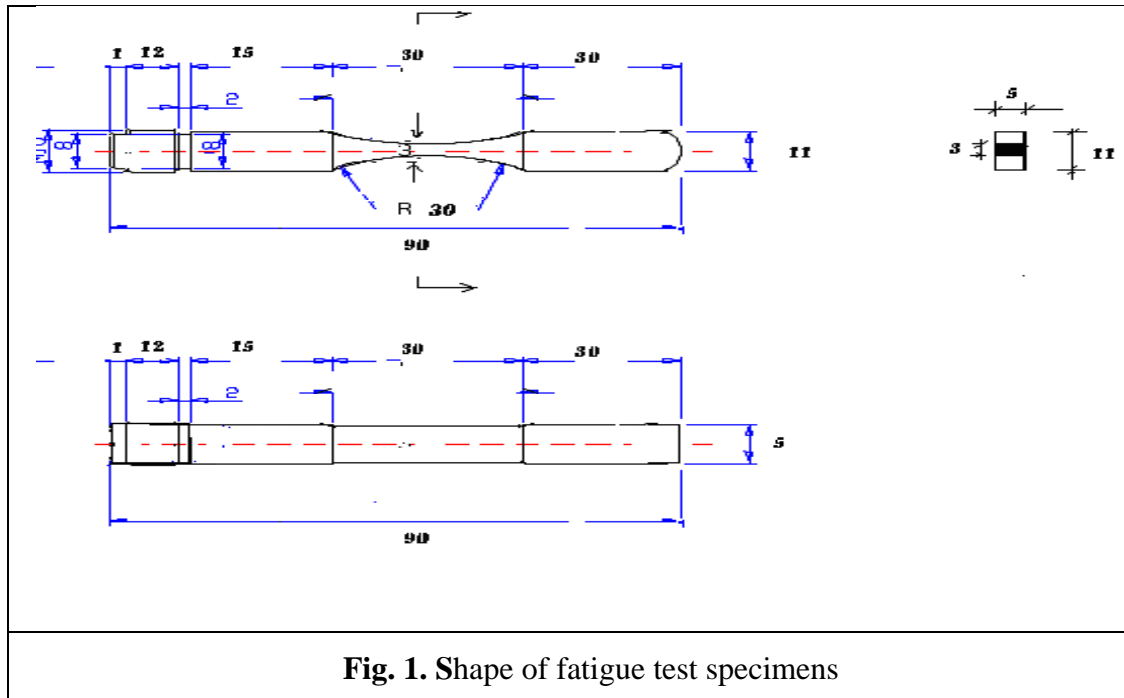
Two basic powder grades were used for this investigation. One was a water atomized iron powder pre-alloyed with 1.5% Cr and 0.2% Mo (Astaloy CrL, Höganäs AB). Another was a water atomized iron powder pre-alloyed with 1.5% Mo (Astaloy Mo, Höganäs AB). Carbon was admixed to both materials as natural graphite (Kropfmühl UF4). Amide wax was used as lubricant. The mixed powders were compacted into test bars which were sintered at 1120°C for 30 minutes, in a 90% N<sub>2</sub> - 10% H<sub>2</sub> atmosphere. The cooling rate was approx. 0.8°C/s. The range of sintered density was 7.1g/cm<sup>3</sup> ~7.5g/cm<sup>3</sup>. The detailed information is listed in **Table 1**.

TABLE1: List of investigated materials

Material composition (code)	Sintering temperature / °C	Sintered density / g/cm <sup>3</sup>	Porosity / %
AstCrL+0,6%C+0,7%C-wax (M. 1)	1120	7.58	3.37
AstCrL+0,6%C+0,7%C-wax (M.2)	1120	7.08	9.81
AstMo+0,6%C+0,7%C-wax (M. 3)	1120	7.5	4.45
AstMo+0,6%C+0,7%C-wax (M. 4)	1120	7.05	10.19

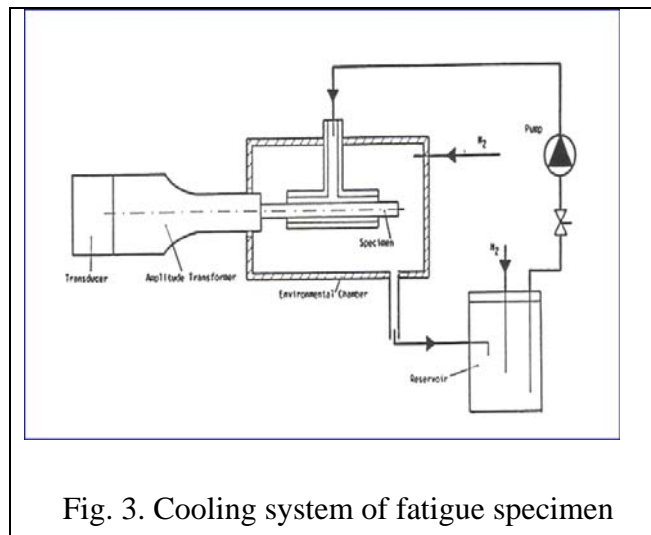
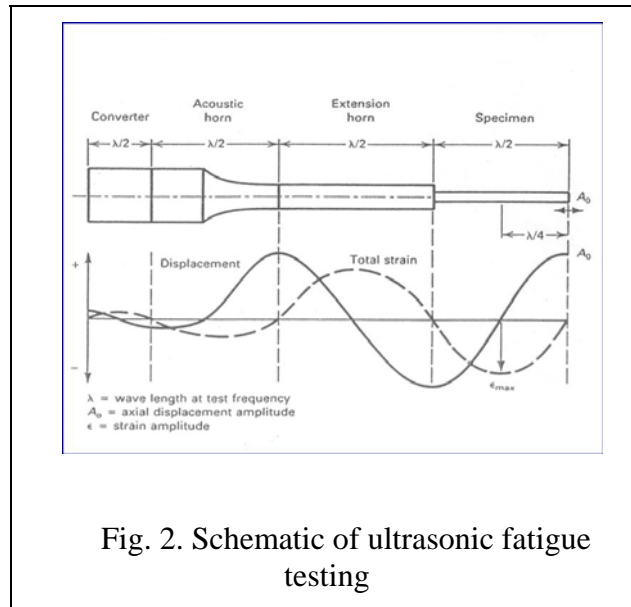
## 2.2. Fatigue specimens

The fatigue specimens (shape according to ISO 3928) were machined to a slightly thinner gauge section by milling with a sharp hard metal tool and turning the thread on one end; then the gauge section was longitudinally ground and the edges slightly rounded. The specimens were screwed into the tester and fatigue loaded at approx. 20 kHz in a push-pull mode at  $R = -1$ , cooling being afforded by pumping a drilling emulsion around the specimen. The specimen drawing is shown in Fig. 1.



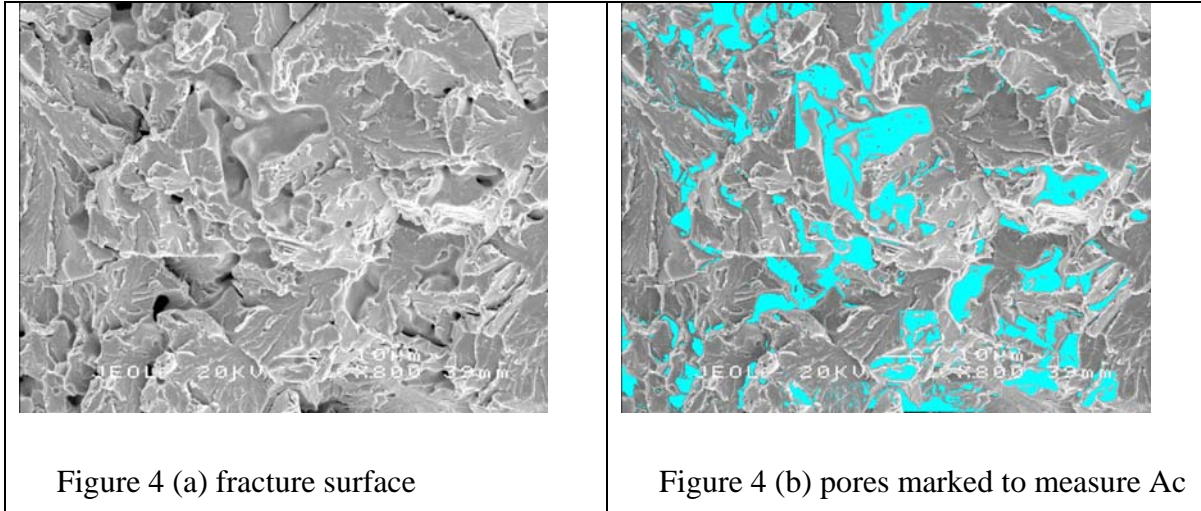
### 2.3. Ultrasonic Resonance Fatigue System

The principle of the ultrasonic resonance fatigue system is as follows: Acoustic resonance is developed in the converter by application of the electrical excitation provided by the power supply. The converter generates a standing acoustic wave that produces a cyclic displacement at the end of the converter. The acoustic wave proceeds down the rest of the resonant wave train to the specimen, the dimension of the specimen being adapted to its Young's modulus in such a way that a displacement node, i.e. a stress peak, is generated in the centre of the gauge section, the entire test assembly being a resonating system. The variation of the displacement and strain amplitudes along the wave train is shown in Fig. 2. Roth [3] The cooling system of testing specimen is shown in Fig. 3.



## 2.4. Measuring Method for the Load-Bearing Area

For investigation of load bearing area, the notched standard specimens were fractured by impact loading at  $-196^{\circ}\text{C}$  so that the plastic deformation was reduced and the fracture surfaces depicted the original, i.e. undeformed, microstructure. The fracture surfaces were investigated by SEM, 9 photographs being taken from each fracture surface. The locations where the 9 photographs were taken were distributed evenly on the fracture surface. The load-bearing area  $A_c$  was determined on these photographs using an image analyzing system Danninger [4].  $A_c$  was defined as the total area of fractured material bridges as a fraction of the image area. The image analyzing system was an improved system based on the semiautomatic VIDS-III image analysis system in which the Polygon Converting Scan-line Algorithm Wylie et al [5] was used to measure  $A_c$ . In this image analyzing system not only Polygon Converting Scan-line Algorithm but also Seed Filling Algorithm Levoy[6] was used so that the measuring speed was increased greatly. The gray value in the spot where the mouse pointed to on the photograph can be shown on the interface, and the range of gray scale can be selected while using the Seed Filling Algorithm so that the accuracy of results can be enhanced. The results could be computed automatically. Figure 4. (a) shows the fracture surface of a low-porosity specimen obtained by impact loading at  $-196^{\circ}\text{C}$ . Figure 4 (b). shows pores marked by the software for  $A_c$  measurement.



## 3. Results and Discussion

Material composition (code)	Fatigue Strength / MPa	UTS / MPa	Fatigue strength ratio	Ac
AstCrL+0,6%C+0,7%C-wax (M.1)	310	1033	0.3	0.93
AstCrL+0,6%C+0,7%C-wax (M. 2)	170	801	0.21	0.66
AstMo+0,6%C+0,7%C-wax (M. 3)	230	775	0.29	0.84
AstMo+0,6%C+0,7%C-wax (M.4)	110	597	0.18	0.4

Table 2. Results List

The results of mechanical testing and Ac values were listed in Table 2. The relationship between fatigue strength ratio FS / UTS and Ac is shown in Figure 5. The virtually linear correlation is clearly visible.

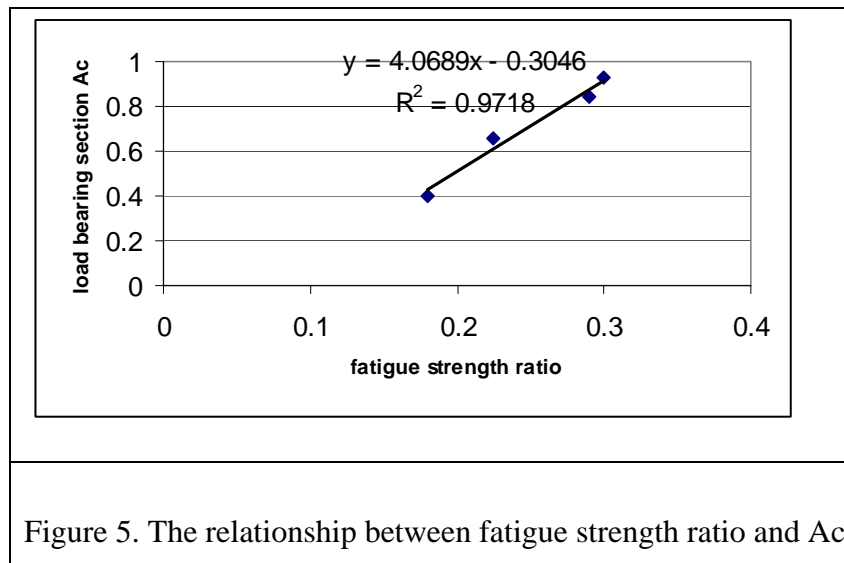


Figure 6. shows a typical fatigue fracture topography. In our investigation it could be observed that crack initiation always occurred at the surface of the specimens. But the exact location of crack initiation is difficult to be recognised, see Figure7. This may be explained by the fact that crack nucleation may have occurred independently at several sites where



- More investigations of the relationship between fatigue strength and Ac in sintered steels should be carried out.

## Acknowledgement

This work was carried out in the international project “Höganäs Chair”. The authors thank Höganäs AB, Sweden, for financial support.

## References

1. B. Weiss, et al: “*High Cycle Fatigue Behaviour of Iron Based PM Materials*” MPR March 1990.
2. H. Danninger et al: “*Microstructure and Mechanical Properties of Sintered Iron*” pmi vol. 25, no.3, 1993.
3. L.D. Roth: “*Ultrasonic Fatigue Testing*” on proceeding of the first international conference on ultrasonic fatigue testing.
4. H. Danninger: “*Characterization of Pressed and Sintered Ferrous Materials by Quantitative Fractography*” Prakt. Metallogr. 31(1994) 2.
5. C. Wylie et al: “*Halftone Perspective Drawings by Computer*” Proceeding of the Fall Joint Computer Conference 67, Thompson Books, Washington,DC, 1967.
6. M. Levoy, “*Area Flooding Algorithms*”, Computer Graphics, 16(3), July 1982, ACM SIGGRAPH, New York.
7. S.J. Polasik et al “*Fatigue Crack Initiation and Propagation in Ferrous PM alloys*” Proceeding PM2TEC June, 2002 Orlando.
8. Laz, P.J. et al “*Fatigue Life Prediction From Inclusion Initiated Cracks*,” International Journal of Fatigue, 1997
9. Lindqvist, B.: “*Influence of Microstructure and porosity on fatigue properties of Sintered Steels*” Metal powder Report (1989), 443-448.
10. Sonsino, C.M.: “*Influence of as-sintered material strength on the improvement of fatigue behavior by surface rolling*” PM’90 London, July 1990.
11. Tengzelius, J.: “*High Density PM Steels for Fatigue Loaded Parts*” Höganäs intern report PM96-7.
12. Beiss, P.: “*Fatigue Strength of Sintered Steels*” Horizons of Powder Metal (1986), 491-494.
13. Bergmark, A.: “*Fatigue Crack Initiation in PM Steels*”, Proceeding PM2TEC June, 2002 Orlando.

